Article

Cell Reports

The SAGA Deubiquitination Module Promotes DNA Repair and Class Switch Recombination through ATM and DNAPK-Mediated γH2AX Formation

Graphical Abstract

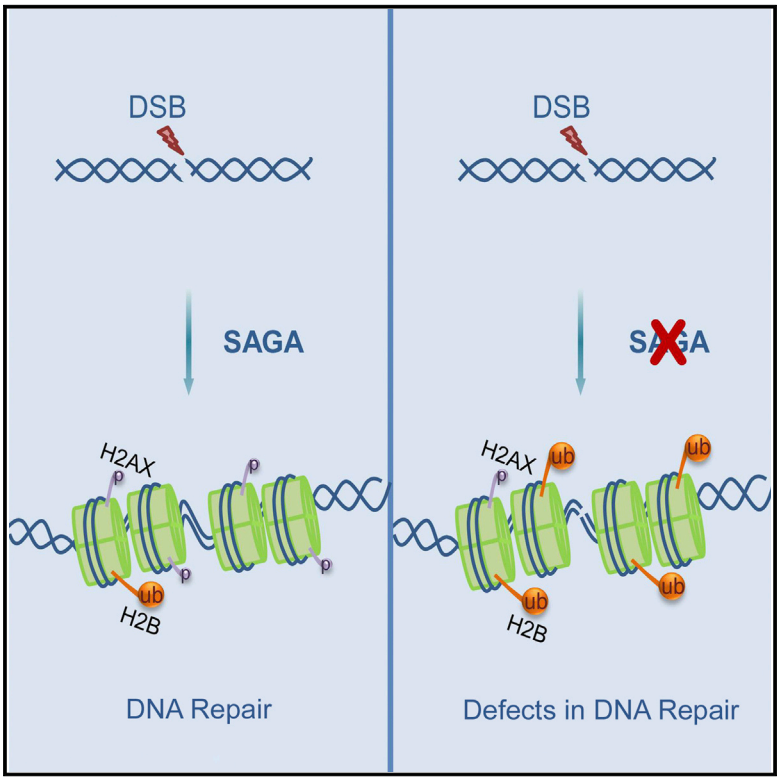

Authors

Shaliny Ramachandran, Dania Haddad, Conglei Li, ..., Troy Ketela, Jason Moffat, Alberto Martin

Correspondence

alberto.martin@utoronto.ca

In Brief

Activation-induced deaminase induces class switch recombination by inducing DNA breaks at the immunoglobulin locus. Ramachandran et al. showed that the SAGA deubiquitination module is critical for this process. They showed that this complex is required for optimal γH2AX formation and functions upstream of various double-stranded DNA repair pathways.

Highlights

- The SAGA deubiquitinase module functions in class switch recombination
- Deficiency in SAGA deubiquitinase activity impairs double-stranded break repair
- γH2AX formation is compromised in cells deficient in SAGA deubiquitinase activity

Ramachandran et al., 2016, Cell Reports *15*, 1554–1565
May 17, 2016
http://dx.doi.org/10.1016/j.celrep.2016.04.041

OPEN ACCESS
CellPress

Cell Reports
Article

The SAGA Deubiquitination Module Promotes DNA Repair and Class Switch Recombination through ATM and DNAPK-Mediated γH2AX Formation

Shaliny Ramachandran,[1,5] Dania Haddad,[1,5] Conglei Li,[1,5] Michael X. Le,[1,5] Alexanda K. Ling,[1] Clare C. So,[1] Rajeev M. Nepal,[1] Jennifer L. Gommerman,[1] Kefei Yu,[2] Troy Ketela,[3] Jason Moffat,[4] and Alberto Martin[1,*]
[1]Department of Immunology, University of Toronto, Medical Sciences Building, Toronto, ON M5S 1A8, Canada
[2]Department of Microbiology and Molecular Genetics, Michigan State University, East Lansing, MI 48824, USA
[3]Princess Margaret Genomics Centre, University Health Network, Toronto, ON M5G 1L7, Canada
[4]Donnelly Centre and Banting and Best Department of Medical Research, University of Toronto, Toronto, ON M5S 1A8, Canada
[5]Co-first author
*Correspondence: alberto.martin@utoronto.ca
http://dx.doi.org/10.1016/j.celrep.2016.04.041

SUMMARY

Class switch recombination (CSR) requires activation-induced deaminase (AID) to instigate double-stranded DNA breaks at the immunoglobulin locus. DNA breaks activate the DNA damage response (DDR) by inducing phosphorylation of histone H2AX followed by non-homologous end joining (NHEJ) repair. We carried out a genome-wide screen to identify CSR factors. We found that Usp22, Eny2, and Atxn7, members of the Spt-Ada-Gcn5-acetyltransferase (SAGA) deubiquitination module, are required for deubiquitination of H2BK120ub following DNA damage, are critical for CSR, and function downstream of AID. The SAGA deubiquitinase activity was required for optimal irradiation-induced γH2AX formation, and failure to remove H2BK120ub inhibits ATM- and DNAPK-induced γH2AX formation. Consistent with this effect, these proteins were found to function upstream of various double-stranded DNA repair pathways. This report demonstrates that deubiquitination of histone H2B impacts the early stages of the DDR and is required for the DNA repair phase of CSR.

INTRODUCTION

B cells switch from expressing the IgM class of antibody to IgG, IgE, or IgA classes by a process termed class switch recombination (CSR). CSR requires the enzyme activation-induced deaminase (AID) to catalyze the deamination of deoxycytidines in the immunoglobulin switch regions, thus creating G:U pairs (Stavnezer et al., 2008). These AID-induced mutations are processed by the mismatch repair and base excision repair pathways, leading to the generation of staggered double-stranded DNA breaks (DSBs) at the donor and acceptor switch regions (Kracker and Durandy, 2011). These DNA breaks instigate a signaling cascade analogous to the DNA damage response (DDR) elicited by irradiation-induced DNA damage (Daniel and Nussenzweig, 2013). Repair of the DSBs in a manner that places the acceptor switch region adjacent to the recombined VDJ segment, while deleting the intervening DNA, results in CSR (Chaudhuri and Alt, 2004). This repair process is primarily completed during the G_1 phase of cell cycle and largely depends on non-homologous end joining (NHEJ) and to a lesser extent on alternative end-joining (A-EJ) (Han and Yu, 2008; Yan et al., 2007). DSBs are recognized by DDR sensors, one such example being MRN, which then recruits ATM, which in turn phosphorylates S/TQ motifs on an array of substrates, key among which is histone H2AX (Petersen et al., 2001; Stiff et al., 2004). Phosphorylated H2AX, denoted γH2AX, then recruits various factors culminating in the localization of 53BP1 and Rif1 on histone H2A near the DSB to promote NHEJ (Bothmer et al., 2010; Di Virgilio et al., 2013; Zimmermann et al., 2013).

Histone H2B has also been implicated in the response to DNA damage (Moyal et al., 2011). Irradiation-induced DNA damage results in the recruitment of the RNF20/40 E3 ubiquitin ligase heterodimer to DSBs to catalyze mono-ubiquitination of histone H2B at K120 in mammals (Moyal et al., 2011; Shiloh et al., 2011). H2BK120ub (hereafter referred to as H2Bub) is thought to initiate chromatin disassembly, providing access to both NHEJ and homologous recombination (HR) DNA repair factors (Fierz et al., 2011; Moyal et al., 2011). H2Bub can be engaged by a component of the SAGA module that catalyzes deubiquitination of H2Bub (Daniel et al., 2004; Henry et al., 2003). SAGA is composed of multiple independent modules. For example, one component of the SAGA module can mediate histone acetylation (Zhang, 2003) and requires the Gcn5-containing module, while deubiquitination is mediated by another component of SAGA that requires the enzyme Usp22, as well as structural components Eny2, Atxn7, and Atxn7L3 (Lang et al., 2011; Zhao et al., 2008). Although Eny2 is found in different complexes such as the THO complex that can alter R-loop stability and maintain genomic stability (Domínguez-Sánchez et al., 2011; Ruiz et al., 2011), Usp22 has so far only been shown to mediate deubiquitination (Daniel et al., 2004; Henry et al., 2003). Previous studies have suggested that SAGA may play a role in global nucleotide excision repair within chromatin (Martinez

et al., 2001), and recent work has shown that deubiquitination of H2B is required for transcription-coupled repair in response to UV-induced RNA polymerase II stalling (Mao et al., 2014). However, H2Bub and factors involved in the formation and removal of this histone mark have not been implicated in the CSR process.

Although the accumulated knowledge on DSB repair is vast and complex, this knowledge is likely to be incomplete. As CSR employs multiple known DNA repair factors, this suggested that a screen based on CSR might reveal factors of more general significance to the DDR. Moreover, a screen based on CSR poses the potential advantage that CSR requires that all steps in the DSB repair process be completed. As described in this report, we carried out a genome-wide loss-of-function RNAi screen, which identified Eny2 as a candidate gene involved in CSR. More detailed analyses showed that Usp22, Eny2, and Atxn7, components of the SAGA deubiquitinase module, are required for efficient CSR and DSB repair, as well as for maintaining the steady-state level of H2Bub. Elevated levels of H2Bub as a result of Usp22 or Eny2 deficiency interfere with γH2AX formation, which likely occurs through interference with ATM and DNAPK activity. Consistent with a role in the early stages of the DDR, Usp22 and Eny2 act upstream of DNA repair and are required for efficient HR, NHEJ, and A-EJ. Our results suggest that H2Bub added by RNF20/40 must be actively removed in order to complete CSR and DSB repair.

RESULTS

To gain further insights into the CSR process, we performed a loss-of-function, genome-wide RNAi screen to identify factors that function in CSR. We used the mouse cell line, CH12F3-2 (referred to as CH12) that undergoes CSR from IgM to IgA after stimulation with a cocktail composed of anti-CD40, IL-4, and TGFβ (CIT) (Nakamura et al., 1996). As described in the Experimental Procedures section, we used a previously described lentiviral small hairpin (sh)RNA library containing ~78,000 hairpins targeting ~16,000 murine genes, where each shRNA vector bears puromycin resistance and a unique barcode. The transduced cells were incubated with puromycin for 3 days and then stimulated for 3 days with the CIT cocktail. The cells were then sorted for surface IgA expression. The abundance of each shRNA hairpin in the IgA-negative population relative to that in the IgA-positive population was measured by microarray (Figure 1A). There were 1,070 hairpins that were enriched by ≥1.75-fold in the IgA-negative population over the IgA-positive population (Figure 1B) and were thus considered as candidate CSR factors. Two of the 1,070 hairpins targeted AID (ranked 186 and 221) and both reduced AID expression (Figure 1E) and CSR (Parsa et al., 2012). To assess the validity of the screen, we tested a subset of these candidates in individual assays, which showed that 64% of the candidate factors inhibited CSR (Figures 1C and 1D) and, of this subgroup, ~70% also reduced AID protein levels (Figure 1E). The remainder of the hairpins had no effect on AID protein levels while inhibiting CSR. One of these hairpins targeted the Eny2 gene and was selected for further characterization.

The SAGA Deubiquitinase Module Promotes CSR Downstream of AID Activity

Eny2, Atxn7, and Usp22 are components of the SAGA deubiquitination module. Hence, we assessed whether shRNA-mediated knock down of Eny2, Atxn7, and Usp22 in CH12 cells led to a decrease in CSR. We identified four shRNAs directed against these components that knocked down the respective mRNAs at different levels (Figure 2A). All shRNAs reduced CSR to IgA in CIT-stimulated CH12 cells at 48 hr post stimulation (Figures 2B and S1A). Because the shEny2-2 vector knocked down Eny2 transcript more than the other vectors targeting components of the SAGA deubiquitinase module, most subsequent experiments were performed using the shEny2-2 hairpin, henceforth termed shEny2. ShEny2 maintained knock down of CSR in CH12 cells over a 3-day period following stimulation (Figure 2C). Expression of a shRNA-resistant Eny2-cDNA expression vector in an Eny2-knockdown clone rescued both Eny2 transcript levels (Figure 2E) and CSR (Figure 2D). These experiments gave rise to many clones with altered levels of steady-state Eny2 mRNA. Using these clones, we found that CSR to IgA strongly correlated with Eny2 transcript levels (Figure 2E).

We also edited exon 2 of the *Usp22* gene in CH12 cells using CRIPSR/Cas9 and generated two distinct Usp22 knockout clones (i.e., Usp22 KO-1 and KO-2) due to frameshift mutations, as revealed by Usp22 exon 2 sequencing (Figure S1B). Usp22 mRNA levels were reduced in these Usp22 KO clones, likely due to nonsense mediated RNA decay (Figure 2F). The mRNA levels of Usp22 were partially reduced in one Usp22-het clone, which had a frameshift mutation in one allele and a 27 nucleotide deletion (or nine amino acid deletion) in the other allele (Figure S1B). CSR to IgA was reduced by ~60% in the Usp22-KO clones at 48 hr and over 72 hr (Figures 2G and 2H), but not in the Usp22-het clone. Furthermore, ex vivo spleen mouse B cells transduced with shEny2 also demonstrated a reduced ability to undergo CSR, in this case, to IgG1 (Figure 2I).

Eny2- or Usp22-knockdown did not alter AID expression or germline transcripts at the μ and α switch regions in CH12 cells (Figures 3A and 3B). AID expression was similar in the Usp22-KO-1 clone and lower in the Usp22-KO-2 clone compared to the wild-type (WT) clone (Figures 3A and S2A). The variable expression of AID in these clones is consistent with the finding that different subclones of CH12 express AID and switch at slightly different levels from each other (Figure S2B). To determine whether Usp22-deficiency affected AID function at the switch region, we sequenced the 5′μ switch region in Usp22-WT and -KO clones. The results show that the AID mutation frequency was consistent with the AID levels in these clones and that Usp22-deficiency does not impair AID function (Table 1).

To further test whether the SAGA deubiquitinase functions independently of AID, we induced CSR from IgM to IgA in $AID^{-/-}$ CH12 cells using the CRISPR/Cas9 system by targeting the Cas9 endonuclease to regions immediately upstream and downstream of the μ and α switch regions, respectively. The $AID^{-/-}$ cell line was achieved by knocking out exons 2–4 of the AID gene by HR (Figures S2C–S2E). Using these $AID^{-/-}$ CH12 cells, we found that Eny2-, Atxn7-, and Usp22 knockdown led to a ~30% reduction in CRISPR/Cas9-mediated CSR compared to controls (Figures 3C and S2F). We also performed the

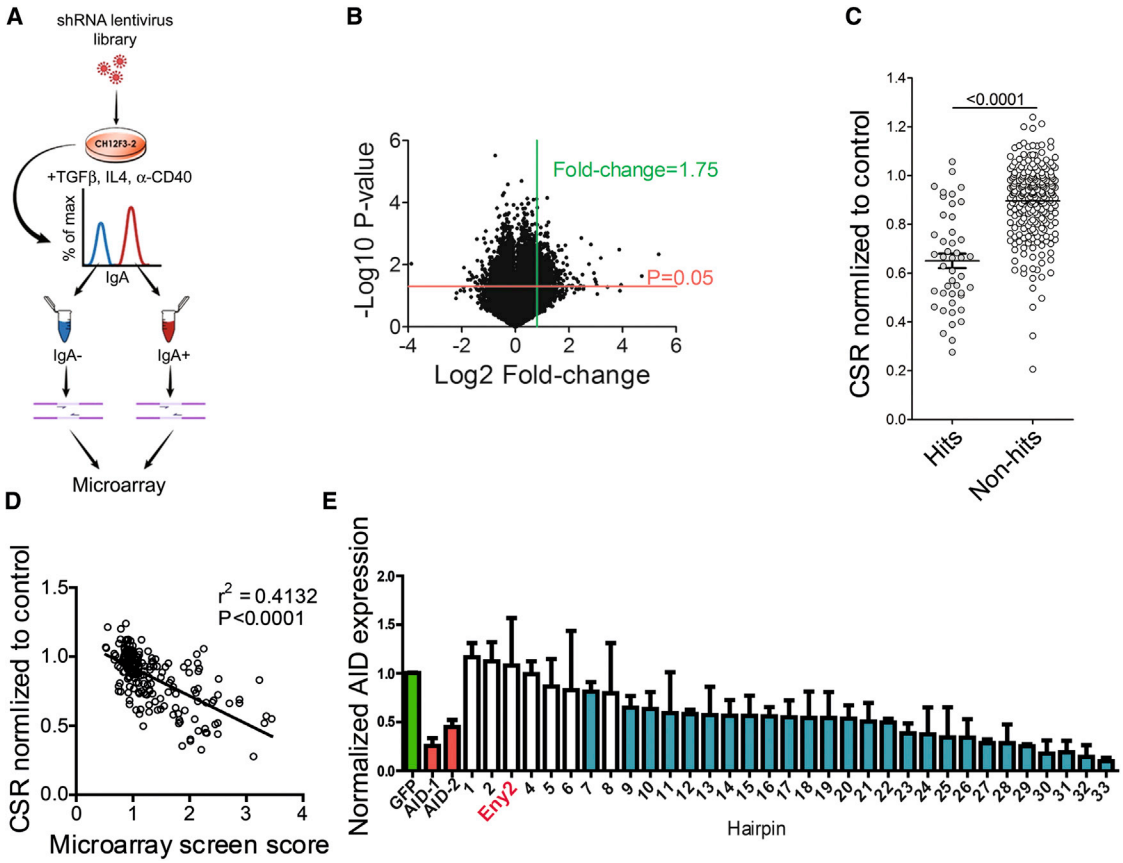

Figure 1. RNAi Screen Reveals Eny2 as a Candidate CSR Factor likely Acting Downstream of AID

(A) Screen methodology. The CH12 cells were transduced with a pooled mouse lentiviral shRNA library. As described in the Experimental Procedures section, positively transduced cells were selected for puromycin resistance, stimulated to undergo CSR, and stained for surface IgA (in three biological replicates). The population of switched (IgA+) and non-switched (IgA−) cells were separated by FACS. Genomic DNA was extracted from each population for PCR-mediated amplification of the shRNA barcode, which was then subjected to microarray analysis to determine the representation of each hairpin in each population. For each hairpin, the CSR screen score was determined as fold difference of hairpin representation in IgA− population over IgA+ population.

(B) Volcano plot analysis. For each hairpin, the p value was determined using paired, two-tailed Student's t test analysis between the hairpin representations in the IgA− population versus the IgA+ population. The negative log (to the base 10) of the p value was calculated and plotted on the y axis. For each hairpin, the log (to the base 2) of the CSR screen score (fold difference of the hairpin level in IgA− population relative to the IgA+ population) was calculated and plotted on the x axis.

(C) Validation analysis. There were 45 hairpins identified as a hit (score $\geq$1.75) and 230 non-hit hairpins (score <1.75) that were selected for validation analysis. The ability of each hairpin to affect CSR was individually tested and normalized to a control shRNA targeting GFP set in parallel. The validation analysis revealed a 9.1% false-negative rate and a 35.6% false-positive rate. Each shRNA was tested with two biological replicates and the experiment was performed once.

(D) Correlation analysis. The normalized CSR levels of each hairpin (obtained from the validation analysis) are displayed on the y axis, and the CSR screen score is displayed on the x axis.

(E) AID protein level was determined by western blot analysis in a selected group of 33 screen hits. Of the 33 hairpins identified to target potential CSR factors by the screen, 26 hairpins reduced AID expression (shown in blue), compared to the negative control (shGFP: green) and the positive control (shAID1,2: red). Each shRNA was tested with two biological replicates and the experiment was performed once.

CRISPR/Cas9-mediated CSR in Usp22-KO clones and found a similar defect when compared to controls (Figure 3D); in this experiment, there was some background CSR (i.e., mock, using empty px330 vector) because these clones were WT for AID. These data suggest that the CSR defect in SAGA-deubiquitinase-deficient CH12 cells lies downstream of AID function.

Eny2-knockdown or deletion of Usp22 led to a minor defect in proliferation in CIT-stimulated CH12 cells (Figures S3A and S3B), although this defect was more pronounced in the Eny2-knockdown cells. The proliferation defect in Eny2-knockdown cells was manifested by a block in the G_1-S phase transition and an increase in apoptosis in CIT-stimulated CH12 cells (Figures S3C–S3E). These results are consistent with defective repair of DSBs induced by AID in the G_1 phase of the cell cycle in Eny2-knockdown cells. This defect in proliferation was not detectable by carboxyfluorescein succinimidyl ester (CFSE) dilution experiments (Figures S3F and S3G). Nevertheless, the defect in CSR was not due to an impaired rate of proliferation of the IgA^{+ve} population relative to the IgA^{-ve} population in the Eny2 or Atxn7-knockdown clones as shown by comparable levels of CFSE

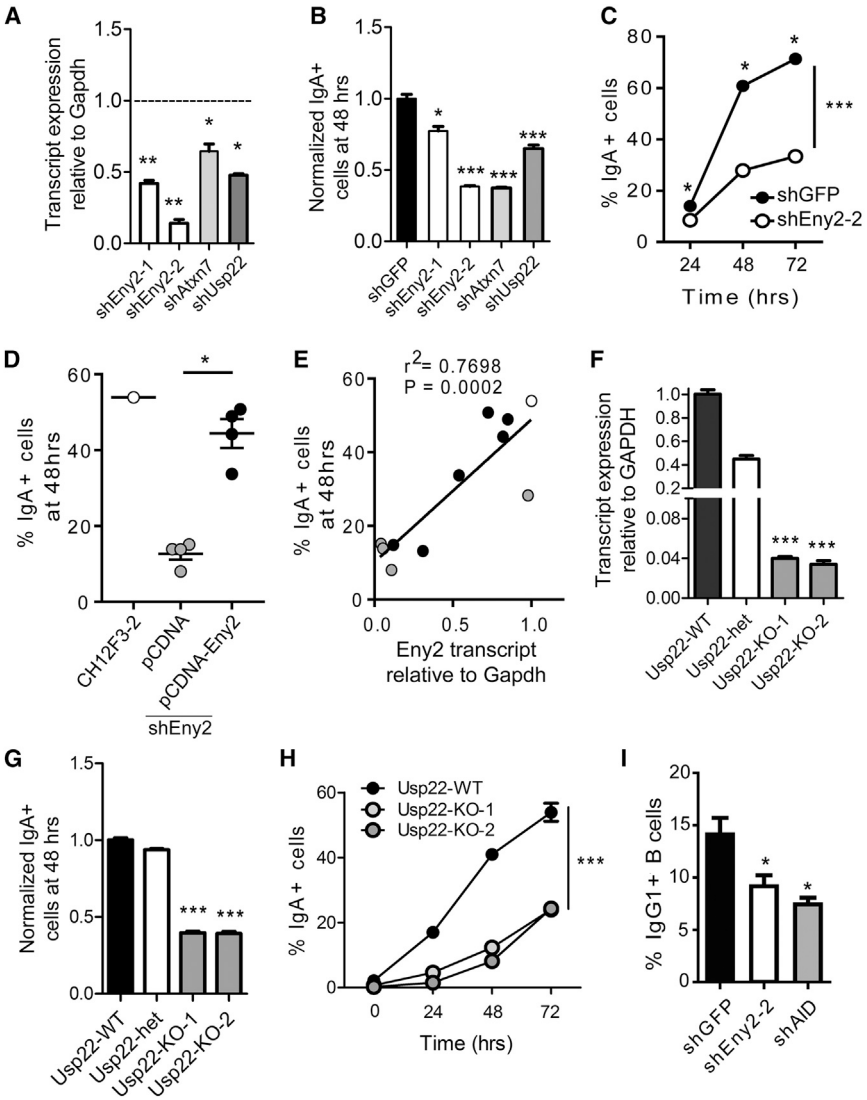

Figure 2. Usp22, Eny2, Atxn7 Are Required for CSR

(A) Eny2, Atxn7, and Usp22 transcript levels relative to GAPDH were determined by qPCR analysis from CH12 cells expressing shEny2-1, shEny2-2, shAtxn7, and shUsp22 compared to the GFP-targeting control shGFP. Each shRNA was tested with two biological replicates.

(B) IgA-expression in 48 hr CIT-stimulated CH12 cells expressing shEny2-1, shEny2-2, shAtxn7, and shUsp22 compared to control shGFP. The experiment was performed with 2–3 biological replicates in two independent experiments.

(C) CSR time course analysis of CH12 cells expressing shEny2 and shGFP. The data were tested by two-way ANOVA. The experiment was performed with three biological replicates.

(D) CSR analysis of clones derived from a CH12 shEny2-knockdown clone transfected with pcDNA3.1 vector control (pcDNA) or transfected with shRNA-resistant Eny2 expression vector (pcDNA-Eny2). The CSR was compared to the parental CH12 clone.

(E) Correlation of CSR and Eny2 transcript levels from clones derived from CH12 shEny2 clone transfected with either pcDNA3.1 control vector or the shRNA-resistant Eny2 expression vector. The gray circles are clones transfected with pcDNA3.1, the black circles are clones transfected with pcDNA-Eny2, and the white circle is the parental CH12 clone. The statistical significance was tested by linear regression analysis. For (D) and (E), each clone was tested with three replicates for qPCR analysis and one experiment for CSR analysis.

(F) Transcript levels as determined by qPCR for Usp22 in the indicated CH12 clones that were subjected to CRISPR/Cas9 editing of the *Usp22* gene (see Figure S1B).

(G) IgA-expression in 48 hr CIT-stimulated WT, het, and KO Usp22 CH12 clones.

(H) CSR time course analysis of WT and KO Usp22 CH12 clones. The data were tested by two-way ANOVA.

(I) CSR analysis of ex vivo mouse spleen B cells expressing shEny2, shAID, and control shGFP. Unless otherwise indicated, all of the data presented in this figure were analyzed by unpaired, two-tailed Student's t test. See also Figure S1.

mean fluorescence intensity between IgA^{+ve} and IgA^{-ve} cells in all populations (Figures S3F and S3G). Collectively, these data support the notion that the SAGA deubiquitinase module is required for efficient CSR downstream of AID activity, nor does the minor proliferation defect account for the more significant defect in CSR.

The SAGA Deubiquitinase Module Is Required for Deubiquitination of H2Bub in CH12 Cells in Response to Ionizing Irradiation

H2Bub has been implicated in DSB signaling and repair (Kari et al., 2011; Moyal et al., 2011; Nakamura et al., 2011). Indeed, H2Bub was increased in CH12 cells subjected to ionizing radiation (Figure 4A), although the rate of H2B ubiquitination is delayed compared to that of ATM-induced γH2AX and phosphorylated Kap1 formation (Figures 4A and S4A–S4C). As discussed above, Usp22, Eny2, and Atxn7 are components of the SAGA module that deubiquitinates H2Bub (Lang et al., 2011). To confirm this function in CH12 cells, we measured whether the level of H2Bub was affected by deletion of Usp22 or knock down of Eny2 or Atxn7. Usp22-KO clones and Eny2-knockdown cells had higher steady-state levels of H2Bub than controls (Figures 4B, 4C, and S4D). There was an even greater increase of H2Bub 3 hr after 8 Gy of irradiation in Usp22-KO clones and in Eny2- and Atxn7-knockdown cells (Figures 4B and S4D–S4F).

We also measured H2Bub in the reconstituted clones, which express different steady-state levels of Eny2 (see Figure 2E). The results showed an inverse correlation between Eny2 transcript levels and H2Bub levels (Figure 4D). Moreover, the frequency of CSR was reduced to ~25% in clones with high levels of H2Bub (defined as those clones that expressed 2.5-fold more H2Bub than parental controls) (Figure 4E). Chromatin

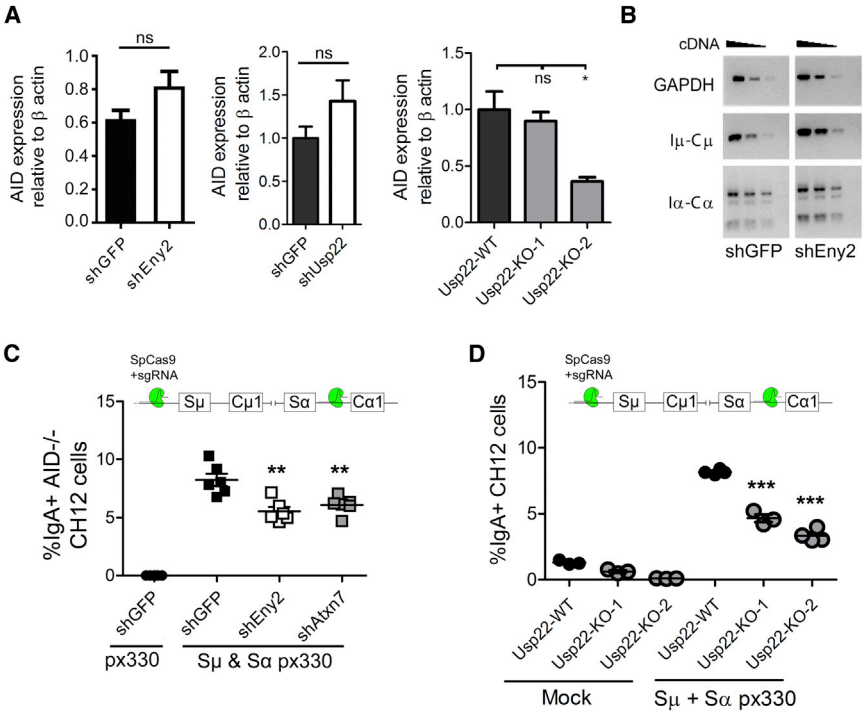

Figure 3. Deficiency in Usp22 and Eny2 Impairs CSR Independent of AID Activity

(A) Expression levels of AID measured by western blot in CH12 cells expressing shGFP, shEny2, and shUsp22 (left and middle). The AID levels in WT and KO Usp22 CH12 clones (right). The AID westerns were performed in 2–4 biological replicates in three independent experiments.

(B) RT-PCR for indicated spliced immunoglobulin sterile transcripts and GAPDH as control in CH12 cells expressing shGFP and shEny2. The RT-PCR analysis was performed with two biological replicates.

(C) CRISPR/Cas9-mediated CSR from IgM to IgA in AID$^{-/-}$ CH12 cells expressing shGFP, shEny2, or shAtxn7. The Cas9 endonuclease was targeted to regions just upstream and downstream of the μ and α switch regions, respectively (Sμ & Sα px300). Px300 represents a Cas9 vector that does not encode a guide RNA.

(D) Same as (C), except that WT and KO Usp22 CH12 clones were used.

See also Figures S2 and S3. All of the data presented in this figure were analyzed by unpaired, two-tailed Student's t test.

immunoprecipitation (ChIP) analysis showed that H2Bub was increased ~3-fold within the Ig μ switch region in Usp22 KO clones and in Eny2 knockdown clones relative to controls (Figures 4F and S4G). Hence, elevated H2Bub at S regions in cells deficient in the SAGA deubiquitinase module will likely have a direct effect on CSR, although we cannot exclude the possibility that global alterations of H2Bub may also affect CSR. These data show that the deubiquitinase activity of the SAGA module regulates the level of H2Bub in response to DNA damage and that failure to remove this histone mark leads to impaired CSR.

Accumulation of H2Bub Interferes with γH2AX Formation

Given the evidence that the SAGA deubiquitinase module functions in the DNA repair phase of CSR, we tested whether deficiencies in Usp22 or Eny2 directly affect the DDR. We first tested whether shEny2 affected the phosphorylation of Kap1, p53, and H2AX upon irradiation. Phosphorylation of Kap1-Ser824 and p53-Ser15 is mediated by ATM, ATR, and DNAPK (Lakin and Jackson, 1999; White et al., 2006), while H2AX is phosphorylated primarily by ATM, but also by DNAPK in response to ionizing radiation-induced DSBs (Stiff et al., 2004). By western blot, Eny2 knockdown did not affect phosphorylation of Kap1 or p53, but led to reduced levels of ionizing radiation-induced γH2AX (Figure S5A). Western blots also confirmed reduced ionizing radiation-induced γH2AX in Usp22-KO clones (Figure 4B). In addition, formation of γH2AX foci was impaired in Eny2-knockdown cells and Usp22-KO clones compared to controls (Figures 5A–5C and S5B). These results suggest that deficiency in the SAGA deubiquitinase module interferes with ATM and/or DNAPK-mediated H2AX-phosphorylation.

To determine whether deficiency in Eny2 or Usp22 affects DNAPK-mediated H2AX-phosphorylation, we assessed the effects of the ATM inhibitor KU55933 (ATMi) on γH2AX in cells deficient in Eny2 and Usp22. Cells pre-incubated with the ATMi will largely depend on DNAPK to induce γH2AX upon irradiation. To test the efficacy of the ATMi, we determined the effects of the ATMi on phosphorylation of Kap1 (Kap1-pSer824), a known ATM substrate. As expected, Kap1-pSer824 was reduced by 2-fold with ATMi (Figure S5C). Although a previous report showed that ATM phosphorylates RNF20/40 to induce H2Bub (Moyal et al., 2011), we found that the levels of H2Bub were not greatly affected with ATMi (Figure S5C). In the presence of ATMi, the numbers of γH2AX foci were reduced in the Eny2-knockdown cells and Usp22-KO clones compared to controls (Figures 5D and 5E). Hence, deubiquitination of histone H2Bub is required for a normal DNAPK-mediated γH2AX response.

To test the possibility that elevated H2Bub also interferes with ATM-mediated phosphorylation of H2AX, we treated CH12 cells with the DNAPK inhibitor NU7441 (DNAPKi) and examined γH2AX induction upon ionizing irradiation. As expected, using the A70.2 INV-4 cell line that expresses GFP upon RAG1/2-mediated rearrangement (Bredemeyer et al., 2006), DNAPKi was found to reduce the levels of V(D)J recombination (Figure S5D), a process that is dependent on DNAPK (Blunt et al., 1995), and the levels of the DNAPK pS2056, a site phosphorylated by DNAPK itself (Figure S5E). In the presence of 10 μM DNAPKi, γH2AX foci formation was still reduced in the Eny2-knockdown cells and Usp22-KO clones compared to controls (Figures 5D and 5E). These data imply that accumulation of H2Bub leads to impaired ATM and DNAPK activity on H2AX, which in turn limits γH2AX levels and results in reduced CSR.

Table 1. SHM in Switch μ Region in Usp22 KO and Control Cells

	WT	KO1	KO2
Mutations (#)	15	14	7
Nucleotides sequenced (#)	10,128	7,596	8,862
Mutation frequency[a]	1.48×10^{-3}	1.84×10^{-3}	0.79×10^{-3}
Mutations at G:C bases (%)[b]	93	100	100
AID hotspot mutations (%)[c]	60	86	100

[a]Frequency is defined as mutations/bp sequenced.
[b]Percentage of mutations at G:C base pairs calculated over total number of mutations.
[c]Mutations at WRC and GYW motifs. A/T nucleotides = W; A/G nucleotides = R; and T/C nucleotides = Y.

Usp22 and Eny2 Are Required for Optimal NHEJ, A-EJ, and HR

The defect in γH2AX induction suggests that different DSB repair pathways might be affected by H2Bub accumulation. Previous work has shown that RNF20/40, which ubiquitinates H2B at lysine 120, is required for NHEJ- and HR-mediated repair of DSBs (Kari et al., 2011; Moyal et al., 2011; Nakamura et al., 2011). Hence, we tested whether Usp22 and Eny2 are required for HR and NHEJ, as well as A-EJ and single-stranded annealing (SSA) repair. To assess HR, CH12 cells were transfected with the DR-GFP construct that harbors a GFP gene interrupted with an I-SceI site and a truncated GFP repair template for HR-mediated repair (Pierce et al., 1999). HR frequency was then measured in a DR-GFP expressing CH12 clone as the percent of GFP positive cells after transfection of an I-SceI expressing construct. To study repair in the context of the SAGA complex, the CH12 clone containing this construct was transduced with the shLacZ-containing (control) or the shEny2 or shAtxn7-containing lentiviruses. Knockdown of Eny2 and Atxn7 led to a ~50% decrease in HR compared to controls (Figure S6A). The DR-GFP plasmid was also transfected into Usp22-WT and KO clones, selected in bulk, and assessed for GFP expression following transfection with the I-SceI plasmid. The results also show a strong HR defect in both Usp22 KO clones (Figure 6A). Furthermore, we made use of the topoisomerase I inhibitor camptothecin, which induces DSBs that are repaired by HR (Adachi et al., 2004). Consistent with the above result, CH12 cells expressing shEny2 were more sensitive to camptothecin than controls (Figure S6B). To measure the effects of Eny2 on NHEJ, we expressed shEny2 in A70.2 INV-4 cells, which led to a ~25% reduction in GFP expression relative to controls (Figure S6C). NHEJ, A-EJ, and SSA were also measured in the Usp22-WT and KO clones with the EJ5-GFP, EJ2-GFP, and SA-GFP plasmids, respectively (Bennardo et al., 2008; Gunn and Stark, 2012), using the methodology described for the DR-GFP plasmid to generate bulk transfections. The results show that Usp22-deficiency impairs NHEJ, A-EJ, and SSA (Figures 6B–6D). However, there was no specific defect in A-EJ since the average microhomology lengths in μ–α switch junctions were similar between Eny2-knockdown clones and controls in contrast to DNA ligase $IV^{-/-}$ cells that had longer microhomology lengths in the switch junctions (Figures 6E and S6D). These data suggest that the SAGA-deubiquitinase module functions upstream of the end joining phase of CSR. Indeed, we found that knockdown of Eny2 and Atxn7 in DNA ligase $IV^{-/-}$ cells led to a further reduction in CSR (Figure 6F). Collectively, these data show that the deubiquitinase activity of SAGA functions early in the DDR and upstream of multiple different DSB repair pathways.

DISCUSSION

While it is well established that ubiquitination of histone H2A plays a significant role in the DDR and in CSR (Fradet-Turcotte et al., 2013), histone H2B has thus far not been well characterized in this context. In this report, we show that deubiquitination of H2B plays a significant role downstream of AID activity in the DNA repair phase of CSR.

Our report further shows that deubiquitination of H2B facilitates γH2AX formation. A previous report, however, showed that RNF20/40-depletion coupled with a low dose of irradiation did not affect γH2AX formation, but led to persistent γH2AX at later time points (Moyal et al., 2011). Discrepancy between our observations and the previous report could be due to the different biological outcome of accumulated H2Bub (SAGA-deficiency) versus the loss of H2Bub (RNF20/40-deficiency). Our findings are particularly intriguing since we found that the regulatory effect of H2Bub on γH2AX is dependent on both ATM and DNAPK activity. Based on our observation that H2Bub levels peak after γH2AX upon irradiation, a question that arises is how does H2Bub influence γH2AX formation? One possibility is that since cells deficient in Eny2, Atxn7, or Usp22 already exhibit an increase in steady-state H2Bub prior to irradiation, this might interfere with γH2AX formation by ATM and DNAPK. Another possibility is that persistent H2Bub can lead to extensive WSTF-SNF2H-mediated H2A-Y142-phosphorylation (Nakamura et al., 2011; Xiao et al., 2009), which might block recruitment of DNA repair factors such as MDC1 (Cook et al., 2009) that are known to be important for maintaining the γH2AX signal, possibly by protecting the site from phosphatases (Stucki et al., 2005). Nevertheless, the defect in γH2AX in SAGA-deficient cells suggests an early defect in the DDR. In support of this notion, we found that the SAGA deubiquitination module is required for efficient DNA repair by multiple processes including HR, NHEJ, A-EJ, and SSA. Previous studies reported similarly reduced HR and NHEJ activity in RNF20/40 E3 ubiquitin ligase deficient cells (Kari et al., 2011; Moyal et al., 2011; Nakamura et al., 2011).

RNF20/40-mediated ubiquitination of histone H2B and SAGA-mediated deubiquitination of histone H2B were previously implicated in transcription regulation (Weake and Workman, 2008). It was postulated that these H2B ubiquitination/deubiquitination factors that function in transcription are directed toward DSB repair in the context of DNA damage stress (Shiloh et al., 2011). However, it is also possible that H2B ubiquitination/deubiquitination could represent a direct link between transcription and DSB repair, and that H2Bub might recruit DNA repair factors specifically to DSBs within actively transcribed regions of the genome, such as at the immunoglobulin switch regions.

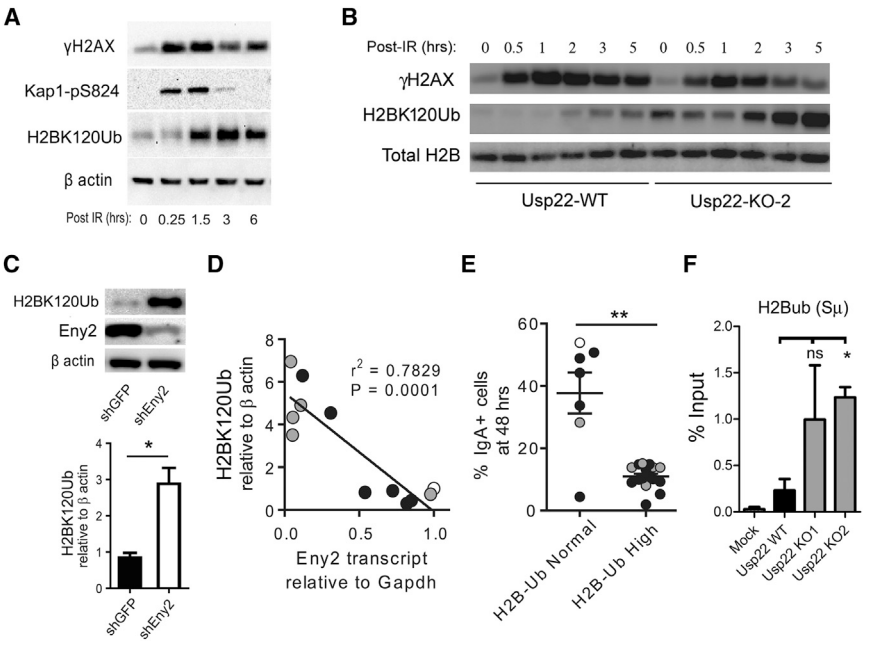

Figure 4. Eny2 and Usp22 Are Required for Deubiquitination of H2Bub in CH12 Cells

(A) Time course analysis of irradiation-induced post translational modifications involved in DDR. CH12 control (shGFP) cells were exposed to 8 Gy of γ-radiation and harvested at various time points for western blot analysis of γH2AX, Kap1-pSer824, and H2Bub, all relative to β-actin. The figure is representative of four biological replicates.

(B) WT or Usp22 KO-2 clones were exposed to 8 Gy of γ-radiation and harvested at various time points for western blot analysis of H2Bub and γH2AX. A representative blot of two independent experiments is displayed.

(C) Representative western blot analysis (top) and compiled data (bottom) on steady-state levels of H2Bub and Eny2 relative to β actin in CH12 cells expressing shGFP and shEny2.

(D) Correlating H2Bub levels to Eny2 transcript levels in the parental clone (white symbol) and clones derived from a CH12 shEny2 clone expressing either pcDNA3.1 vector (gray symbol) or shRNA-resistant Eny2 expression vector (black symbol) from Figure 2D. The statistical significance was tested by linear regression analysis.

(E) CSR analysis on CH12 clones with either normal steady-state levels of H2Bub or high (at least ~2.5-fold above the parental CH12 clone) steady-state levels of H2Bub.

(F) H2Bub ChIPs were carried out using sonicated DNA from the 24 hr CIT-stimulated CH12 Usp22 WT and KO clones. qPCR was performed using Sμ primers, which can be found in Table S1. The mock represents a ChIP signal using normal mouse IgG. The data were normalized to the DNA input signals.

See also Figure S4. Unless otherwise indicated, all of the data presented in this figure were analyzed by unpaired, two-tailed Student's t test.

In support of this notion, H2B-deubiquitination has been shown to facilitate transcription-coupled nucleotide excision repair (Mao et al., 2014). Transcription-coupled repair has been shown to be dispensable for somatic hypermutation (SHM) since deficiencies in Cockayne syndrome group A (CSA), a factor involved in transcription-coupled repair, showed no defect in SHM (Jacobs et al., 1998). If the SAGA deubiquitinase module indeed functions in transcription-coupled repair, our work suggests that this DNA repair pathway be reassessed in CSR.

Recent findings have shown a critical role for factors involved in RNA processing in antibody diversification processes (Basu et al., 2011; Pavri et al., 2010; Zheng et al., 2015). These studies showed that these factors function to recruit AID to the immunoglobulin switch region to initiate CSR. Interestingly, members of the SAGA histone acetylation module have been shown to interact with the RNA exosome (Tous et al., 2011). However, it is unlikely that the SAGA deubiquitinase activity functions in this manner during CSR since targeting of AID to the switch region is normal in Usp22-deficient CH12 cells (Table 1), and the effect of SAGA deficiency was independent of AID activity (Figures 3C and 3D). Nevertheless, these data do not preclude the possibility that AID together with RNA processing/splicing machinery and the SAGA deubiquitinase module collaborate to facilitate repair of DSBs during CSR. AID has been shown to interact with single-stranded (ss)DNA with a half-life measured in minutes that are atypical for enzymes, raising the possibility that AID persists on immunoglobulin genes after deamination to facilitate the downstream DNA repair processes (Larijani et al., 2007). Indeed, the c-terminal tail of AID has been shown to recruit DDR factors such as CtIP during CSR to facilitate the end joining phase of CSR (Zahn et al., 2014). At this time, it is unclear whether H2B modifications influence the extent of RNA processing/splicing or affect the ability of AID to recruit DNA repair factors that are required for CSR. Nevertheless, these are intriguing possibilities that require further investigation.

In conclusion, we have identified that H2Bub plays a key role in CSR. We further found that deubiquitination of H2Bub by the SAGA module is important for DNAPK and ATM-induced γH2AX formation, and that regulation of this histone mark is necessary for the function of various DSB repair pathways.

EXPERIMENTAL PROCEDURES

Lentiviral shRNA Screen

CH12 cells were grown as described before (Ramachandran et al., 2010). There were 300 million CH12 cells that were transduced with a pooled lentiviral library composed of 77,690 unique shRNA (The RNAi Consortium) (Moffat et al., 2006) at a multiplicity of infection of ~0.2–0.3. Each shRNA harbored a puromycin resistant gene and a barcode that reveals the identity of the shRNA. Transduced cells were selected with puromycin (1 μg/ml) for 3 days and subsequently stimulated with 1 ng/ml recombinant human TGFβ1 (R&D Systems), 10 ng/ml recombinant mouse IL-4 (R&D Systems), and 2 μg/ml functional grade purified anti-mouse CD40 (eBioscience) for 3 days. Stimulated CH12 cells were subjected to extracellular staining with PE-conjugated anti-mouse IgA (Southern Biotech) and sorted by fluorescence-activated cell sorting (FACS)Aria (BD Biosciences). Genomic DNA was extracted from each of the sorted populations using the Blood Maxi Prep Kit (QIAGEN). shRNA hairpin barcodes were PCR-amplified and used as probes in microarray experiments as described previously (Ketela et al., 2011). shRNA sequences with a high coefficient of variation between technical replicates (CV > 0.3), a low microarray

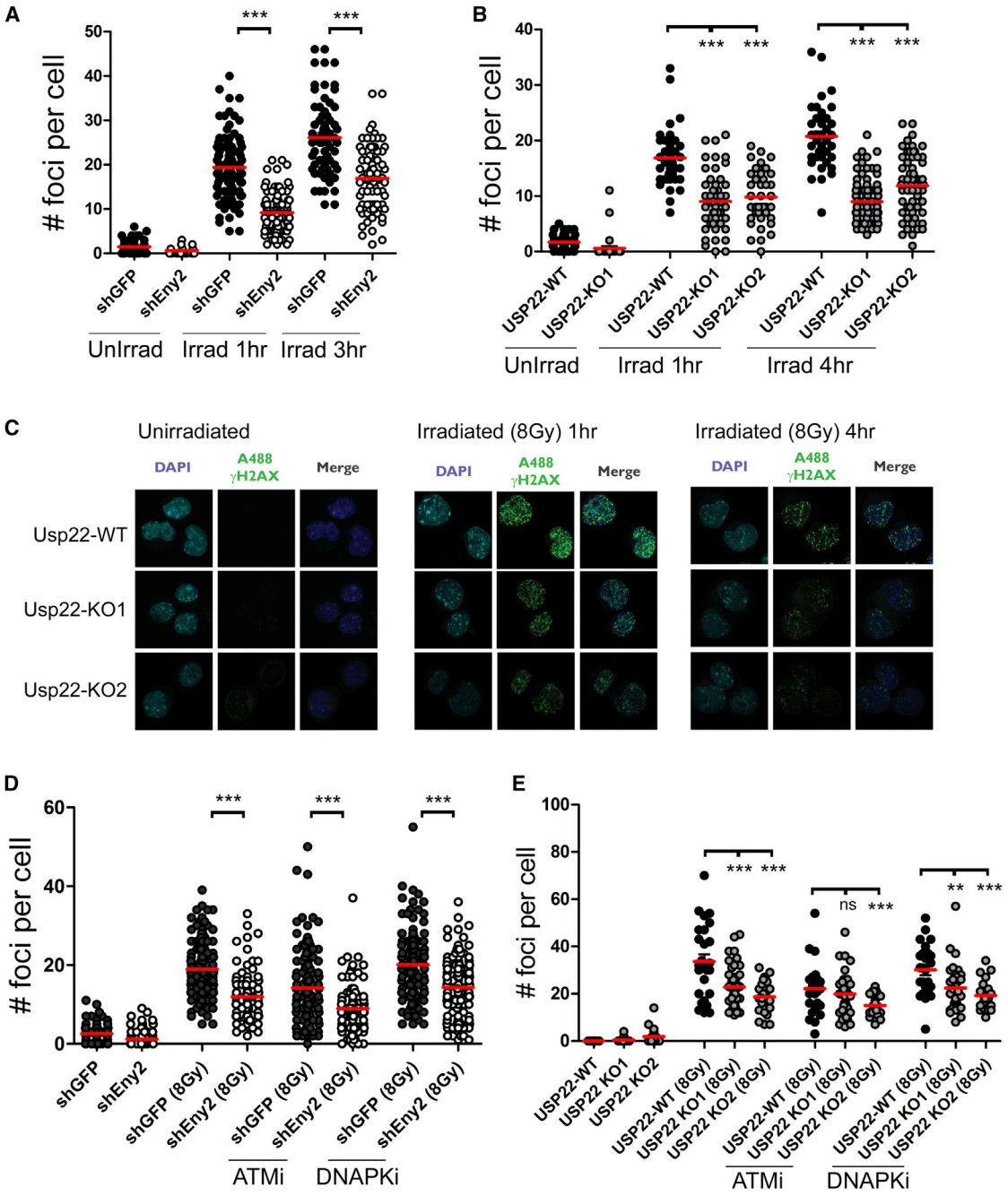

Figure 5. Accumulation of H2Bub Impairs γH2AX Formation

(A) CH12 cells expressing shGFP or shEny2 were exposed to 8 Gy of γ-radiation. The cells were then subjected to γH2AX immunofluorescence analysis. The number of γH2AX foci counted per cell are shown for shGFP (black circles) and shEny2 (white circles) at 1 and 3 hr post irradiation. There were 75 to 100 cells that were analyzed per sample and images are representative of three independent experiments.

(B) Same as (A), except that WT and Usp22-KO clones were analyzed 1 and 4 hr post irradiation. The representative experiment of three experiments is shown.

(C) Representative images of Usp22 WT and KO clones that were exposed to 8 Gy of γ-radiation and subjected to immunofluorescence analysis for γH2AX.

(D) CH12 cells expressing shGFP or shEny2 without or with 10 μM ATMi or 10 μM DNAPKi were exposed to 8 Gy of γ-radiation and subjected to γH2AX immunofluorescence analysis 1 hr post irradiation.

(E) Same as (D), except that WT and Usp22-KO clones were analyzed without or with pre-treatment of ATMi or DNAPKi.

See also Figure S5. All of the data presented in this figure were analyzed by unpaired, two-tailed, Student's t test.

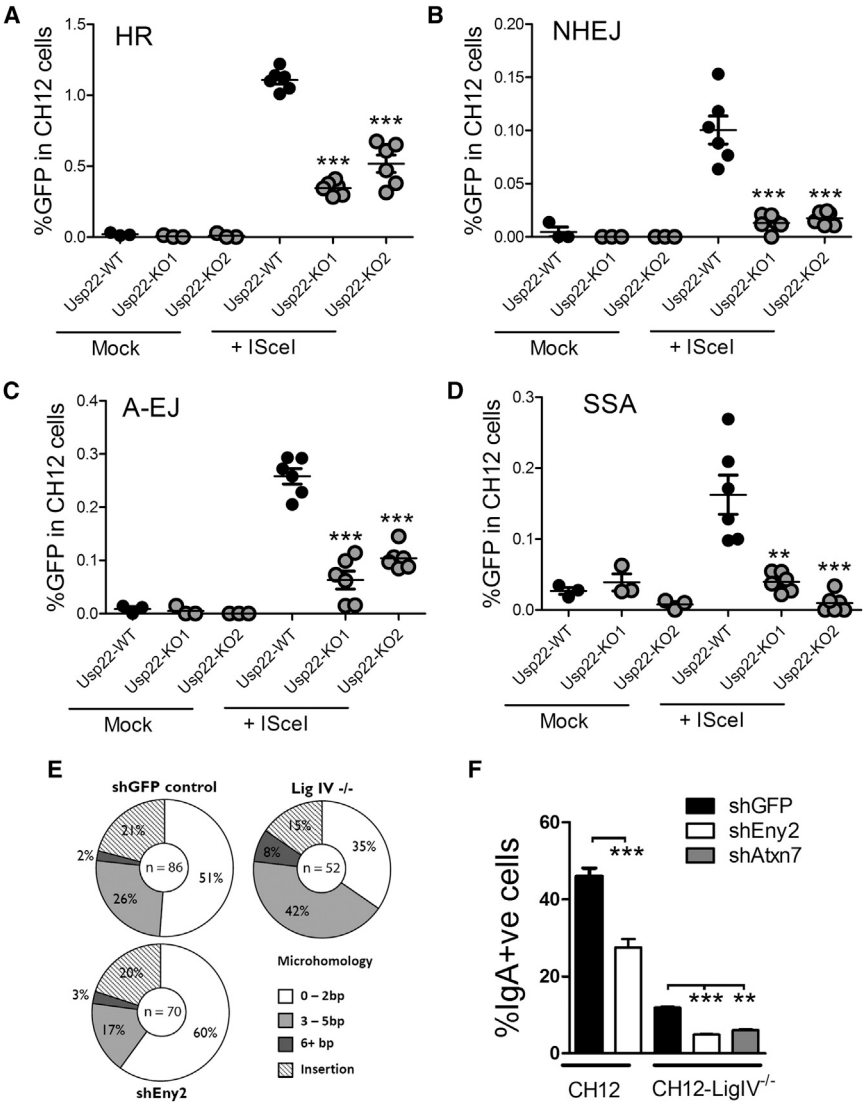

Figure 6. Usp22 Functions Upstream of Known DSB Repair Pathways

(A–D) Usp22 WT and KO clones were transfected with DR-GFP plasmid to measure HR (A), EJ5-GFP plasmid to measure NHEJ (B), EJ2-GFP plasmid to measure A-EJ (C), and SA-GFP plasmid to measure SSA (D) and were then mock transfected or transfected with the I-SceI expression plasmid to induce cleavage of the transgenes and then subjected to flow cytometry for GFP expression.

(E) Lengths of microhomologies in Sμ/Sα junctions cloned from IgA-switched CH12 cells expressing shGFP or shEny2, or Ligase IV-deficient CH12 (LigIV$^{-/-}$). Sμ/Sα junctions are arranged according to microhomology usage: near-blunt joins (0–2 bp, white), joins with microhomology (3–5 bp, light gray and 6+ bp, dark gray), or insertions (dashed). The data are pooled together from two independent experiments.

(F) CSR analysis of CH12 cells and CH12-LigIV$^{-/-}$ expressing shGFP, shEny2, and shAtxn7 was performed after CIT-stimulation for 48 hr. The data are representative of three replicates performed in three independent experiments.

See also Figure S6. Unless otherwise indicated, all of the data presented in this figure were analyzed by unpaired, two-tailed Student's t test.

signal (Signal < 10), and a high coefficient of variation between biological replicates (CV > 0.4) were eliminated, leaving 58,127 shRNA sequences for further analysis. Screen score for individual shRNAs was defined as mean IgA-negative microarray signal divided by mean IgA-positive signal. Hairpins with a screen score ≥1.75 (which represents a *Z* score of 1.99) were deemed as hits.

In Vitro Cell Culture

CH12 cells were maintained and CSR assays were performed as described previously (Ramachandran et al., 2010). Briefly, cells were stimulated with 1 ng/ml recombinant human TGFβ1 (R&D Systems), 10 ng/ml recombinant mouse IL-4 (R&D Systems), and 2 μg/ml functional grade purified anti-mouse CD40 (eBioscience) for various time points and analyzed by flow cytometry, as described below. Negative control lentiviral shRNA constructs including shGFP (TRCN0000072181), shLacZ (TRCN0000072223), shLuc (TRCN0000072243), and candidate shRNA including shEny2 (TRCN0000086039 and TRCN0000086041), shAtxn7 (TRCN0000104973), and shUsp22 (TRCN0000030812) were used from The RNAi Consortium. CH12 cells were transduced with lentivirus for 24 hr on 24-well plates for bulk transductions or diluted and plated on 96-well plates to obtain clones. Positively transduced cells were selected with 1 μg/ml puromycin for 3 days.

For growth curve analysis, CH12 cells were diluted to a concentration of 1 × 10^5 cells/ml and aliquoted on a 96-well plate. At various time points, the numbers of live-trypan blue excluded cells were counted using a haemocytometer. AID$^{-/-}$ and Ligase IV$^{-/-}$ CH12 cells were generated as described previously (Han and Yu, 2008). ATMi and DNAPKi were obtained from Tocris Bioscience. CH12 cell lines were irradiated with various doses of γ-radiation using a Gammacell 1000 Irradiator and not preincubated or incubated with 10 μM ATMi or 10 μM DNAPKi. The GFP expressing A70.2 INV-4 cells were transduced with shLacZ and shEny2 lentivirus and selected with hygromycin. Naive A70.2 INV-4 cells were treated with DMSO or 5 μM DNAPKi. For RAG induction, positively selected cells were treated with 3 μM imatinib at 0.25 × 10^6 cells/ml. At 4 days after induction, GFP positive cells were analyzed by flow cytometry.

Generation of Usp22$^{-/-}$ CH12 Cells Using CRISPR/Cas9

The CRISPR guide RNA sequence against exon 2 of murine Usp22 (sgUsp22: TCTGCGGCATCCACCTGAAC) was designed with publically available software derived from: http://www.crispr.mit.edu. The sgUsp22 was cloned into the px459 (Cas9-2A-puro) vector, sequenced, and electroporated into CH12 cells. The electroporated cells were then plated at a concentration of 0.3 cells/well and single clones of CH12 cells were first screened via T7E1 mismatch cleavage assay, followed by sequencing. Usp22 WT clone was derived from a T7E1 mismatch negative clone, while Usp22-het, KO-1, and KO-2 clones were identified by sequencing T7E1 mismatch positive clones. A more detailed protocol can be found here: https://benchling.com/protocols/5DmqRd/crispr-mediated-gene-disruption-in-ch12f3-2-cells.

Flow Cytometry Analysis

For CSR analysis, CH12 cells were stained with PE-conjugated anti-mouse IgA (Southern Biotech), and ex vivo mouse B cells were stained with PE-conjugated anti-mouse IgG1 antibody clone A85-1 (BD Biosciences). For cell cycle analysis, cells were incubated with 10 μM BrdU for 1 hr followed by ethanol

fixation overnight. Cells were then washed and incubated in 2 M HCl for 30 min, washed and stained with FITC-conjugated anti-BrdU antibody clone PRB-1 (eBiosciences), and then washed and incubated in 20 μg/ml propidium iodide (PI) and 10 μg/ml RNase A for 30 min. For apoptosis analysis, CH12 cells were surface stained for Annexin V using an Annexin V-APC Apoptosis Detection Kit (eBiosciences). Stained cells were analyzed by FACSCalibur (BD Biosciences), Fortessa (BD Biosciences), and FlowJo software (Tree Star).

RT-PCR and Quantitative PCR Analysis

RNA extraction was performed using TRIzol (Invitrogen), followed by DNaseI treatment (Fermentas), and reverse transcription with either a SuperScript III Kit (Life Technologies) or Maxima Kit (Thermo Scientific) to prepare cDNA. cDNA samples were diluted and subjected to PCR reactions for semiquantitative RT-PCR or quantitative (q)PCR reactions. For semiquantitative PCR, the Iμ-Cμ and Iα-Cα amplification primers used were the same as previously described (Muramatsu et al., 2000), GAPDH primers (GAPDH RTPCR For and Rev) can be found in Table S1. For qPCR analysis, primers for GAPDH (GAPDH qPCR For and Rev), Eny2 (Eny2 qPCR For and Rev), Atxn7 (Atxn7 qPCR For and Rev), and Usp22 (Usp22 qPCR For and Rev) can be found on Table S1.

CRISPR/Cas9-Mediated CSR

A pair of single guide (sg)RNA respectively directed to the 5′ and 3′ regions flanking Sμ and Sα were designed and cloned into px330 (Addgene #42230). To induce Cas9-mediated CSR (unpublished data), one million AID$^{-/-}$ CH12 cells were resuspended with 4 μg each of the 5′-Sμ and 3′-Sα px330 vectors and electroporated with a Gene Pulser electroporator (Bio-Rad). Cells were allowed to recover in growth media for 72 hr before staining with anti-IgA-PE and flow cytometry.

ChIP

shGFP and shEny2 CH12 cells were stimulated for 24 hr with CIT. ChIP was performed using the Magna ChIP Immunoprecipitation Kit (Millipore) according to the manufacturer's instructions. In brief, 5 × 10^6 cells were fixed in the presence of 1% formaldehyde for 10 min at room temperature. The reaction was stopped by the addition of glycine to a final concentration of 0.125 M. A soluble chromatin fraction containing fragmented DNA of 200–500 bp was obtained after cell lysis and sonication. IP was performed by incubating the lysate with 5 μg of H2Bub (Millipore) antibody. The immunoprecipitated DNA was subjected to detection by qPCR normalized to the amount of input followed by the maximum value in each data set. Primers used to amplify a sequence upstream of Sμ can be found in Table S1.

Western Blot Analyses

γH2AX (Millipore), H2Bub (Millipore), H2B (Abcam), Kap1-pS824 (Cell Signaling), p53-pS15 (Cell Signaling), AID (Cell Signaling), Eny2 (Santa Cruz), and β actin (Sigma) antibodies were used as specified by the manufacturers' protocols.

Immunofluorescence Staining and Confocal Microscopy

Cells were irradiated with 0 or 8 Gy of gamma radiation (Gammacell 1000) 1 hr prior to cytospin preparation onto poly-L-lysine slides. Cytospin preparations were fixed with 4% paraformaldehyde/PBS. Then, slides were permeabilized with 0.25% (v/v) Triton X-100/PBS followed by blocking with 0.1% Tween + 1% BSA/PBS for 1 hr at room temperature. Slides were incubated with the following primary antibodies (γH2AX, Millipore and Cell Signaling) and secondary antibodies (anti-mouse IgG1 Alexa-488 and anti-mouse Ig H$^+$L Alexa-555, Life Technologies). Following antibody incubation, slides were then incubated with DAPI (0.5 μg/ml, Sigma) and mounted with aqueous mounting media (M1289, Sigma). Images were taken with a confocal microscope (AZ-C2+, Nikon) equipped with a 100× magnification oil immersion lens. Images were acquired and merged within Nikon NIS Elements software and exported for analysis with ImageJ (NIH). For quantification of foci formation, between 75 and 125 cells were counted for number of foci each per shRNA treatment per experiment.

DNA Repair Substrate Assays

For the HR repair substrate analysis, CH12 cells were transfected with 5 μg of the HR reporter DR-GFP (Jasin Lab, Addgene) via electroporation and selected with 1 μg/ml puromycin 24 hr post transfection. shRNA targeting LacZ or Eny2 were derived onto the pLKOTRC005-Hygro vector and transduced into the DR-GFP expressing CH12 clone. Following hygromycin selection (2 mg/ml), 5 μg of pCBASceI (Jasin Lab, Addgene) were transfected into the shRNA-harboring clones and GFP expression was determined 48 hr post transfection by flow cytometry. For Usp22 WT or KO clones, DR-GFP, EJ5-GFP (Addgene), EJ2-GFP (Addgene), or SA-GFP (Addgene) plasmids were electroporated into Usp22 WT and KO clones and selected with puromycin (1 μg/ml) in bulk, followed by transfection with pCBASceI. GFP-positive cells were detected by flow cytometry at 3 days following ISce-I electroporation.

Statistical Analysis

All analyses were performed on GraphPad Prism. For Student's t tests, linear regression analysis, and two-way ANOVA, p values of 0.05 or less were considered significant: *$p < 0.05$, **$p < 0.01$, and ***$p < 0.001$. All error bars represent SD.

SUPPLEMENTAL INFORMATION

Supplemental Information includes Supplemental Experimental Procedures, six figures, and one table and can be found with this article online at http://dx.doi.org/10.1016/j.celrep.2016.04.041.

AUTHOR CONTRIBUTIONS

S.R., D.H., C.L., and M.X.L. conceived and performed experiments and helped write the manuscript. A.K.L. and C.C.S. carried out a few experiments. R.M.N. and T.K. helped to carry out the screen. J.L.G. conceived of some experiments and helped write the manuscript. K.Y. generated the AID$^{-/-}$ CH12 cells. J.M. carried out the screen and helped write the manuscript. A.M. conceived of the experiments and wrote the manuscript.

ACKNOWLEDGMENTS

We are grateful to Maribel Berru for technical help; to Drs. Daniel Durocher, Cristina Escribano-Diaz, James Carlyle, Marc Shulman, and Sagar Sengupta and the Martin laboratory for helpful discussions about this work; to Barry Sleckman for the A70.2 INV-4 cells; to Maria Jasin for the HR substrate; and to Jeremy Stark for the NHEJ, A-EJ, and SSA substrates. This research is supported by a grant from the Canadian Institutes of Health Research (MOP66965) to A.M.

Received: November 11, 2015
Revised: February 26, 2016
Accepted: April 5, 2016
Published: May 5, 2016

REFERENCES

Adachi, N., Iiizumi, S., So, S., and Koyama, H. (2004). Genetic evidence for involvement of two distinct nonhomologous end-joining pathways in repair of topoisomerase II-mediated DNA damage. Biochem. Biophys. Res. Commun. *318*, 856–861.

Basu, U., Meng, F.L., Keim, C., Grinstein, V., Pefanis, E., Eccleston, J., Zhang, T., Myers, D., Wasserman, C.R., Wesemann, D.R., et al. (2011). The RNA exosome targets the AID cytidine deaminase to both strands of transcribed duplex DNA substrates. Cell *144*, 353–363.

Bennardo, N., Cheng, A., Huang, N., and Stark, J.M. (2008). Alternative-NHEJ is a mechanistically distinct pathway of mammalian chromosome break repair. PLoS Genet. *4*, e1000110.

Blunt, T., Finnie, N.J., Taccioli, G.E., Smith, G.C., Demengeot, J., Gottlieb, T.M., Mizuta, R., Varghese, A.J., Alt, F.W., Jeggo, P.A., and Jackson, S.P. (1995). Defective DNA-dependent protein kinase activity is linked to V(D)J recombination and DNA repair defects associated with the murine scid mutation. Cell *80*, 813–823.

Bothmer, A., Robbiani, D.F., Feldhahn, N., Gazumyan, A., Nussenzweig, A., and Nussenzweig, M.C. (2010). 53BP1 regulates DNA resection and the choice between classical and alternative end joining during class switch recombination. J. Exp. Med. *207*, 855–865.

Bredemeyer, A.L., Sharma, G.G., Huang, C.Y., Helmink, B.A., Walker, L.M., Khor, K.C., Nuskey, B., Sullivan, K.E., Pandita, T.K., Bassing, C.H., and Sleckman, B.P. (2006). ATM stabilizes DNA double-strand-break complexes during V(D)J recombination. Nature *442*, 466–470.

Chaudhuri, J., and Alt, F.W. (2004). Class-switch recombination: interplay of transcription, DNA deamination and DNA repair. Nat. Rev. Immunol. *4*, 541–552.

Cook, P.J., Ju, B.G., Telese, F., Wang, X., Glass, C.K., and Rosenfeld, M.G. (2009). Tyrosine dephosphorylation of H2AX modulates apoptosis and survival decisions. Nature *458*, 591–596.

Daniel, J.A., and Nussenzweig, A. (2013). The AID-induced DNA damage response in chromatin. Mol. Cell *50*, 309–321.

Daniel, J.A., Torok, M.S., Sun, Z.W., Schieltz, D., Allis, C.D., Yates, J.R., 3rd, and Grant, P.A. (2004). Deubiquitination of histone H2B by a yeast acetyltransferase complex regulates transcription. J. Biol. Chem. *279*, 1867–1871.

Di Virgilio, M., Callen, E., Yamane, A., Zhang, W., Jankovic, M., Gitlin, A.D., Feldhahn, N., Resch, W., Oliveira, T.Y., Chait, B.T., et al. (2013). Rif1 prevents resection of DNA breaks and promotes immunoglobulin class switching. Science *339*, 711–715.

Domínguez-Sánchez, M.S., Barroso, S., Gómez-González, B., Luna, R., and Aguilera, A. (2011). Genome instability and transcription elongation impairment in human cells depleted of THO/TREX. PLoS Genet. *7*, e1002386.

Fierz, B., Chatterjee, C., McGinty, R.K., Bar-Dagan, M., Raleigh, D.P., and Muir, T.W. (2011). Histone H2B ubiquitylation disrupts local and higher-order chromatin compaction. Nat. Chem. Biol. *7*, 113–119.

Fradet-Turcotte, A., Canny, M.D., Escribano-Díaz, C., Orthwein, A., Leung, C.C., Huang, H., Landry, M.C., Kitevski-LeBlanc, J., Noordermeer, S.M., Sicheri, F., and Durocher, D. (2013). 53BP1 is a reader of the DNA-damage-induced H2A Lys 15 ubiquitin mark. Nature *499*, 50–54.

Gunn, A., and Stark, J.M. (2012). I-SceI-based assays to examine distinct repair outcomes of mammalian chromosomal double strand breaks. Methods Mol. Biol. *920*, 379–391.

Han, L., and Yu, K. (2008). Altered kinetics of nonhomologous end joining and class switch recombination in ligase IV-deficient B cells. J. Exp. Med. *205*, 2745–2753.

Henry, K.W., Wyce, A., Lo, W.S., Duggan, L.J., Emre, N.C., Kao, C.F., Pillus, L., Shilatifard, A., Osley, M.A., and Berger, S.L. (2003). Transcriptional activation via sequential histone H2B ubiquitylation and deubiquitylation, mediated by SAGA-associated Ubp8. Genes Dev. *17*, 2648–2663.

Jacobs, H., Fukita, Y., van der Horst, G.T., de Boer, J., Weeda, G., Essers, J., de Wind, N., Engelward, B.P., Samson, L., Verbeek, S., et al. (1998). Hypermutation of immunoglobulin genes in memory B cells of DNA repair-deficient mice. J. Exp. Med. *187*, 1735–1743.

Kari, V., Shchebet, A., Neumann, H., and Johnsen, S.A. (2011). The H2B ubiquitin ligase RNF40 cooperates with SUPT16H to induce dynamic changes in chromatin structure during DNA double-strand break repair. Cell Cycle *10*, 3495–3504.

Ketela, T., Heisler, L.E., Brown, K.R., Ammar, R., Kasimer, D., Surendra, A., Ericson, E., Blakely, K., Karamboulas, D., Smith, A.M., et al. (2011). A comprehensive platform for highly multiplexed mammalian functional genetic screens. BMC Genomics *12*, 213.

Kracker, S., and Durandy, A. (2011). Insights into the B cell specific process of immunoglobulin class switch recombination. Immunol. Lett. *138*, 97–103.

Lakin, N.D., and Jackson, S.P. (1999). Regulation of p53 in response to DNA damage. Oncogene *18*, 7644–7655.

Lang, G., Bonnet, J., Umlauf, D., Karmodiya, K., Koffler, J., Stierle, M., Devys, D., and Tora, L. (2011). The tightly controlled deubiquitination activity of the human SAGA complex differentially modifies distinct gene regulatory elements. Mol. Cell. Biol. *31*, 3734–3744.

Larijani, M., Petrov, A.P., Kolenchenko, O., Berru, M., Krylov, S.N., and Martin, A. (2007). AID associates with single-stranded DNA with high affinity and a long complex half-life in a sequence-independent manner. Mol. Cell. Biol. *27*, 20–30.

Mao, P., Meas, R., Dorgan, K.M., and Smerdon, M.J. (2014). UV damage-induced RNA polymerase II stalling stimulates H2B deubiquitylation. Proc. Natl. Acad. Sci. USA *111*, 12811–12816.

Martinez, E., Palhan, V.B., Tjernberg, A., Lymar, E.S., Gamper, A.M., Kundu, T.K., Chait, B.T., and Roeder, R.G. (2001). Human STAGA complex is a chromatin-acetylating transcription coactivator that interacts with pre-mRNA splicing and DNA damage-binding factors in vivo. Mol. Cell. Biol. *21*, 6782–6795.

Moffat, J., Grueneberg, D.A., Yang, X., Kim, S.Y., Kloepfer, A.M., Hinkle, G., Piqani, B., Eisenhaure, T.M., Luo, B., Grenier, J.K., et al. (2006). A lentiviral RNAi library for human and mouse genes applied to an arrayed viral high-content screen. Cell *124*, 1283–1298.

Moyal, L., Lerenthal, Y., Gana-Weisz, M., Mass, G., So, S., Wang, S.Y., Eppink, B., Chung, Y.M., Shalev, G., Shema, E., et al. (2011). Requirement of ATM-dependent monoubiquitylation of histone H2B for timely repair of DNA double-strand breaks. Mol. Cell *41*, 529–542.

Muramatsu, M., Kinoshita, K., Fagarasan, S., Yamada, S., Shinkai, Y., and Honjo, T. (2000). Class switch recombination and hypermutation require activation-induced cytidine deaminase (AID), a potential RNA editing enzyme. Cell *102*, 553–563.

Nakamura, M., Kondo, S., Sugai, M., Nazarea, M., Imamura, S., and Honjo, T. (1996). High frequency class switching of an IgM+ B lymphoma clone CH12F3 to IgA+ cells. Int. Immunol. *8*, 193–201.

Nakamura, K., Kato, A., Kobayashi, J., Yanagihara, H., Sakamoto, S., Oliveira, D.V., Shimada, M., Tauchi, H., Suzuki, H., Tashiro, S., et al. (2011). Regulation of homologous recombination by RNF20-dependent H2B ubiquitination. Mol. Cell *41*, 515–528.

Parsa, J.Y., Ramachandran, S., Zaheen, A., Nepal, R.M., Kapelnikov, A., Belcheva, A., Berru, M., Ronai, D., and Martin, A. (2012). Negative supercoiling creates single-stranded patches of DNA that are substrates for AID-mediated mutagenesis. PLoS Genet. *8*, e1002518.

Pavri, R., Gazumyan, A., Jankovic, M., Di Virgilio, M., Klein, I., Ansarah-Sobrinho, C., Resch, W., Yamane, A., Reina San-Martin, B., Barreto, V., et al. (2010). Activation-induced cytidine deaminase targets DNA at sites of RNA polymerase II stalling by interaction with Spt5. Cell *143*, 122–133.

Petersen, S., Casellas, R., Reina-San-Martin, B., Chen, H.T., Difilippantonio, M.J., Wilson, P.C., Hanitsch, L., Celeste, A., Muramatsu, M., Pilch, D.R., et al. (2001). AID is required to initiate Nbs1/gamma-H2AX focus formation and mutations at sites of class switching. Nature *414*, 660–665.

Pierce, A.J., Johnson, R.D., Thompson, L.H., and Jasin, M. (1999). XRCC3 promotes homology-directed repair of DNA damage in mammalian cells. Genes Dev. *13*, 2633–2638.

Ramachandran, S., Chahwan, R., Nepal, R.M., Frieder, D., Panier, S., Roa, S., Zaheen, A., Durocher, D., Scharff, M.D., and Martin, A. (2010). The RNF8/RNF168 ubiquitin ligase cascade facilitates class switch recombination. Proc. Natl. Acad. Sci. USA *107*, 809–814.

Ruiz, J.F., Gómez-González, B., and Aguilera, A. (2011). AID induces double-strand breaks at immunoglobulin switch regions and c-MYC causing chromosomal translocations in yeast THO mutants. PLoS Genet. *7*, e1002009.

Shiloh, Y., Shema, E., Moyal, L., and Oren, M. (2011). RNF20-RNF40: A ubiquitin-driven link between gene expression and the DNA damage response. FEBS Lett. *585*, 2795–2802.

Stavnezer, J., Guikema, J.E., and Schrader, C.E. (2008). Mechanism and regulation of class switch recombination. Annu. Rev. Immunol. *26*, 261–292.

Stiff, T., O'Driscoll, M., Rief, N., Iwabuchi, K., Löbrich, M., and Jeggo, P.A. (2004). ATM and DNA-PK function redundantly to phosphorylate H2AX after exposure to ionizing radiation. Cancer Res. *64*, 2390–2396.

Stucki, M., Clapperton, J.A., Mohammad, D., Yaffe, M.B., Smerdon, S.J., and Jackson, S.P. (2005). MDC1 directly binds phosphorylated histone H2AX to

regulate cellular responses to DNA double-strand breaks. Cell *123*, 1213–1226.

Tous, C., Rondón, A.G., García-Rubio, M., González-Aguilera, C., Luna, R., and Aguilera, A. (2011). A novel assay identifies transcript elongation roles for the Nup84 complex and RNA processing factors. EMBO J. *30*, 1953–1964.

Weake, V.M., and Workman, J.L. (2008). Histone ubiquitination: triggering gene activity. Mol. Cell *29*, 653–663.

White, D.E., Negorev, D., Peng, H., Ivanov, A.V., Maul, G.G., and Rauscher, F.J., 3rd. (2006). KAP1, a novel substrate for PIKK family members, colocalizes with numerous damage response factors at DNA lesions. Cancer Res. *66*, 11594–11599.

Xiao, A., Li, H., Shechter, D., Ahn, S.H., Fabrizio, L.A., Erdjument-Bromage, H., Ishibe-Murakami, S., Wang, B., Tempst, P., Hofmann, K., et al. (2009). WSTF regulates the H2A.X DNA damage response via a novel tyrosine kinase activity. Nature *457*, 57–62.

Yan, C.T., Boboila, C., Souza, E.K., Franco, S., Hickernell, T.R., Murphy, M., Gumaste, S., Geyer, M., Zarrin, A.A., Manis, J.P., et al. (2007). IgH class switching and translocations use a robust non-classical end-joining pathway. Nature *449*, 478–482.

Zahn, A., Eranki, A.K., Patenaude, A.M., Methot, S.P., Fifield, H., Cortizas, E.M., Foster, P., Imai, K., Durandy, A., Larijani, M., et al. (2014). Activation induced deaminase C-terminal domain links DNA breaks to end protection and repair during class switch recombination. Proc. Natl. Acad. Sci. USA *111*, E988–E997.

Zhang, Y. (2003). Transcriptional regulation by histone ubiquitination and deubiquitination. Genes Dev. *17*, 2733–2740.

Zhao, Y., Lang, G., Ito, S., Bonnet, J., Metzger, E., Sawatsubashi, S., Suzuki, E., Le Guezennec, X., Stunnenberg, H.G., Krasnov, A., et al. (2008). A TFTC/STAGA module mediates histone H2A and H2B deubiquitination, coactivates nuclear receptors, and counteracts heterochromatin silencing. Mol. Cell *29*, 92–101.

Zheng, S., Vuong, B.Q., Vaidyanathan, B., Lin, J.Y., Huang, F.T., and Chaudhuri, J. (2015). Non-coding RNA generated following lariat debranching mediates targeting of AID to DNA. Cell *161*, 762–773.

Zimmermann, M., Lottersberger, F., Buonomo, S.B., Sfeir, A., and de Lange, T. (2013). 53BP1 regulates DSB repair using Rif1 to control 5′ end resection. Science *339*, 700–704.